

Contrastive Federated Learning with Tabular Data Silos

Achmad Ginanjar ^a, Xue Li ^a, and Wen Hua ^b

^aSchool of Electrical Engineering and Computer Science, The University of Queensland, Australia

^bDepartment of Computing, Hong Kong Polytechnic University, Hong Kong

January 29, 2024

Abstract

Learning from data silos is a difficult task for organizations that need to obtain knowledge of objects that appeared in multiple independent data silos. Objects in multi-organizations, such as government agents, are referred by different identifiers, such as driver’s license, passport number, and tax file number. The data distributions in data silos are mostly non-IID (Independently and Identically Distributed), labelless, and vertically partitioned (i.e., having different attributes). Privacy concerns harden the above issues. Conditions inhibit enthusiasm for collaborative work. While Federated Learning (FL) has been proposed to address these issues, the difficulty of labeling, namely, label costliness, often hinders optimal model performance. A potential solution lies in contrastive learning, an unsupervised self-learning technique to represent semantic data by contrasting similar data pairs. However, contrastive learning is currently not designed to handle tabular data silos that existed within multiple organizations where data linkage by quasi identifiers are needed. To address these challenges, we propose using semi-supervised contrastive federated learning, which we refer to as Contrastive Federated Learning with Data Silos (CFL). Our approach tackles the aforementioned issues with an integrated solution. In CFL, the learning process begins by locally acquiring contrastive representations of the data within each silo. Subsequently, the knowledge is aggregated from other silos through the federated learning algorithm, allowing the CFL to attain a more comprehensive representation. The resulting CFL model can then be combined with supervised methods. The CFL allows the federated learning algorithm to benefit from the knowledge in silos while enhancing supervised accuracy and addressing inconsistencies in data availability caused by unbalanced data. Moreover, the algorithm’s output can be used to train various types of supervised model that leverage available labels. Our experimental results demonstrate that CFL outperforms current methods in addressing these challenges and providing improvements in accuracy. Additionally, we present positive results that showcase the advantages of our contrastive federated learning approach in complex client environments. ¹.

1 Introduction

Many organizations, including governments, have specific presumptions associated with data silos. The presumption is that there is (imaginary) comprehensive global data that reflect an overarching national business process. However, various branches or organizations have distinct operational procedures and local data. Each of these silos is interlinked through a key identifier to construct hypothetical global data. Data within these structures are maintained in a tabular format, as governments require a consistent key identifier for reading and writing data. This identifier comes in the form of objects called quasi identifiers [14] that connect data across silos. This scenario leads to the creation of a distinctive ecosystem of tabular data silos that presents their own set of unique challenges.

Tabular data silos in government present intricate challenges owing to their segmented nature, leading to Non-Independently and Identically Distributed (non-IID) data. Variations are born from differing data collection techniques, temporal dependencies, and class imbalances, which further deter the creation of collaborative machine learning. Data sharing is also impossible due to political correctness and a sense of ownership [28]. These tabular data silos are vertically partitioned, which means

¹Submitted on Artificial Intelligence Journal , Jan 29, 2024, ARTINT-D-24-00098

that collaborative model learning requires some information sharing. Label costliness, the cost of identifying and labeling specific data points that is expensive, intensifies the complexity within these silos. Addressing these challenges requires innovative solutions. In this paper, we focus on the challenges related to tabular data silos in government settings as follows.

- **Data Silos with Vertical Partition.** Data silos with vertical partitioning represent a structural partition. This form of partitioning arranges the data vertically, allocating specific columns to different silos or departments according to the nature of the information. For example, in a government setting, this segregation might categorize sensitive personal information in one silo, financial details in another, and demographic data in another. Collaborative model learning within this silos environment usually includes data sharing directly or indirectly. This vertical partitioning poses a real challenge for collaborative work, including FL.
- **Data Silos with Data Imbalance.** Within data silos, the confluence of Non-Independently and Identically Distributed (non-IID) data and label costliness often leads to data imbalances. The non-IID property is a rather general condition within the data silo. Label costliness is born because labels are expensive to avail. Label creation requires actual events or domain knowledge. Both require time and resources (human or money), which are expensive. This condition leads to label scarcity in the real world. Both conditions decrease the size and quality of the data used for collaborative work, leading to a poor collaborative learning model.
- **An integrated solution.** Government settings necessitate a strong approach due to their intricate political nature. Finding solutions to these issues necessitates straightforward answers that will ensure successful outcomes. Working on each problem independently can lead to further complications, such as debating which solution is superior and how to combine them. It is essential to provide an integrated solution that can tackle both of these difficulties.

Federated Learning (FL), proposed by McMahan [12], is a promising approach for government settings with tabular data silos. It allows for the training of models across multiple sites without compromising privacy. By aggregating local updates without centralizing data, it facilitates collaborative model training, minimizing privacy risks and addressing data distribution variations while also improving the model. Numerous researchers have addressed several main challenges within the federated learning area. Yang *et al.* [24] improved FL security, while Chen *et al.*, Zhang *et al.*, Servetnyk *et al.*, and Wang *et al.* [4, 26, 16, 21] focused on improving FL data quality. Zhao *et al.*, Yang *et al.*, Lubana *et al.*, and Ji *et al.* [9, 2, 7] concentrated on client participation, and Lu *et al.*, MoFan *et al.* [11, 13] focused on mitigating attacks on FL. Despite the many advances, label costliness within tabular data silos remains an issue. A potential solution to address the challenges posed by low labeled data due to label costliness is to use contrastive learning.

Contrastive learning [26, 16, 3, 8] is a machine learning technique that aims to acquire meaningful representations of data by contrasting pairs of positive (similar data points) and negative (dissimilar data points) . With contrastive learning, existing data are self-optimized to support supervised learning. Some research contributions, such as representation learning [26, 16] and contrastive learning [3, 8], have demonstrated how this technique can improve accuracy when working with data with limitations on label availability.

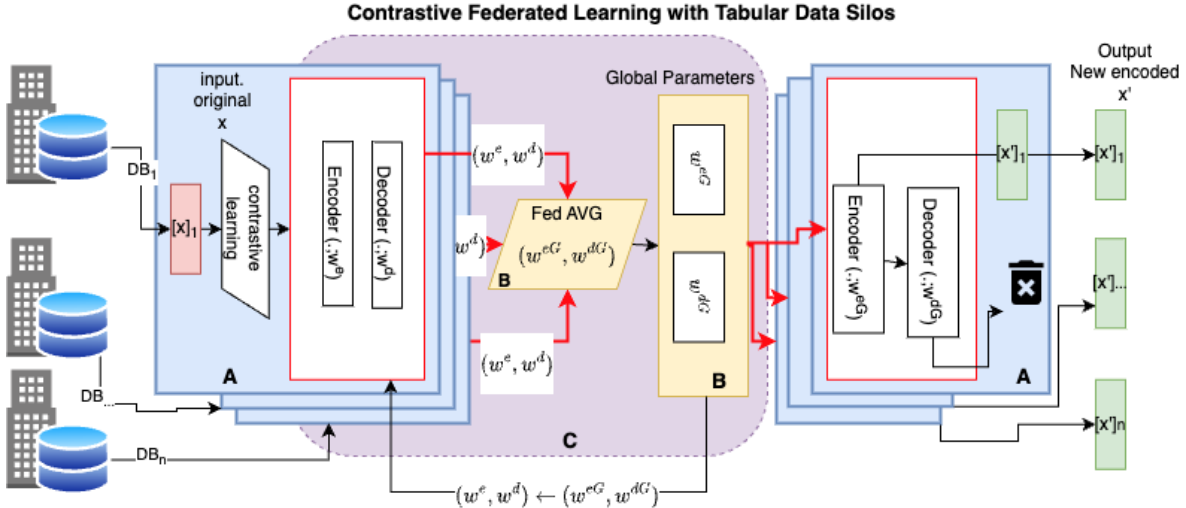


Figure 1: Contrastive Federated Learning with Tabular Data Silos. The (A) areas are local contrastive learning, the (B) area is server learning, and the (C) area is the objects involved in federated learning. $[x]$ is the original data matrix and $[x']$ is the output matrix for supervised inferences.

The current state-of-the-art approaches for contrastive learning usually require data with semantic connections between attributes, such as images, text, or speech. Applying contrastive learning to tabular data is a potential solution, as demonstrated in [20]. However, the previous work was not designed for data silos environments. Previous research concentrated on standard environments without vertical data silos and data imbalance. Existing contrastive learning is not able to capture data with low representation during training in extreme data-unbalance scenarios, such as those addressed in this paper. Nevertheless, this work can be seen as a first attempt at self-supervised learning of tabular data.

We propose a novel approach, Contrastive Federated Learning with Tabular Data Silos (CFL), Figure 1, to address the three challenges mentioned above. This is the first model to apply contrastive learning to tabular data silos in complex scenarios. CFL is designed to handle vertical partition, non-IID, and label costliness within data silos in one comprehensive solution. The core concept revolves around applying contrastive learning principles while leveraging knowledge from all silos. Each silo performs contrastive learning, resulting in an encoder and decoder. The encoder and decoder are then aggregated globally in a global server. The aggregated model benefits from the global differences from the silos. This results in a global encoder and decoder. The global encoder and decoder are then used to continue contrastive learning in each silo. The final result of CFL is an Encoder in each silo. This final encoder encodes new data in each silo with better supervised learning accuracy.

Our proposed CFL introduces two new techniques, namely "null representation" and "tuple representation". The null representation approach guarantees that all silos contain data, even if it is not available. The tuple representation technique is used to adjust contrastive learning to tabular data and silo space. This means that the entire unpartitioned record is used instead of a partial tuple for representation generation, as is done in contrastive learning for images [3]. Using tuple representation during contrastive learning, we can achieve higher accuracy, as demonstrated in Figure 2.

The privacy issue is of utmost importance in the government setting, leading to a reluctance to share data. To address this, our CFL uses federated learning with security features that protect privacy during training and testing. Our CFL requires a set of data with a specific order of identifier keys, raising questions about privacy. However, our CFL maintains data security at the same level as standard FL. Parameters are exchanged in the same way as other FL, without sharing the data. The unique object identifier and the object itself are not shared. Our CFL uses pairs of encoder and decoder for federated learning, but only the encoder is used for the final model. Attacks such as Man in the Middle [1] cannot intercept privacy data, as the parameters do not contain any.

In addition, our model has potential support for multi model setups at the client level. We are the first to apply this method and to substantiate its effectiveness through real-world scenarios. Our

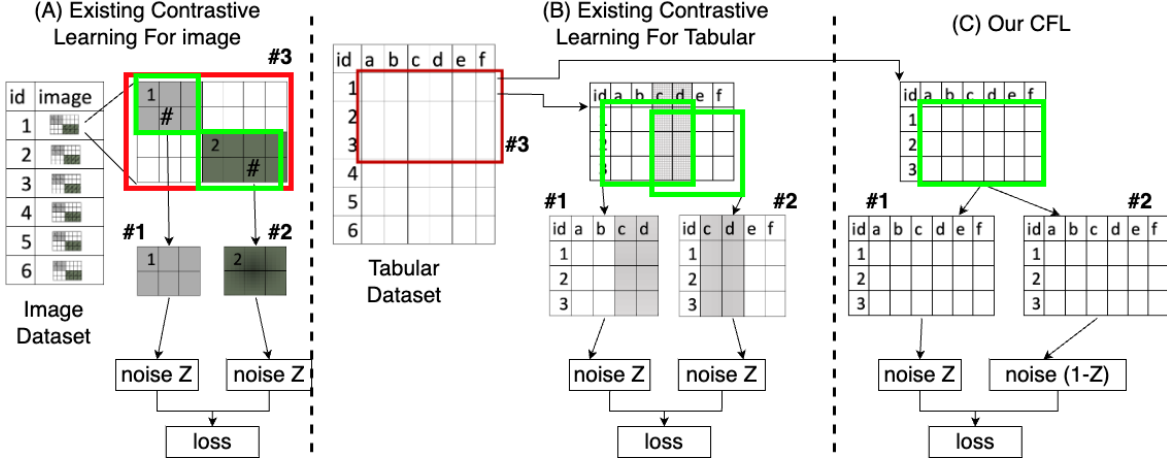


Figure 2: $\{a,b,c,d,e,f\}$ are the column name on tabular data, ($\#1$) is the representation 1^{st} , ($\#2$) is the representation 2^{nd} , and ($\#3$) is a set of data targeted for the loss calculation. In (A), the representations are generated from a **single** record ($\#3$) (single ID). In (B) and (C), the representations are generated from a **set** of records ($\#3$) (several IDs). In (B), the representations are built from part of the data ($\#3$) with some intersection (dark area in B), $\{\#1 \subseteq \#3, \#2 \subseteq \#3, \#1 \cap \#2\}$. In our CFL (C), each representation is a clone of the data ($\#3$), $\{\#3 = \#1 = \#2\}$ / full-row representation.

experiments show better results compared to the existing algorithm.

2 Related Work

2.1 Learning on Vertical Data Silos

Private set intersection (PSI) [10] has been used in vertical federated learning. This technique allows two or more parties to identify the intersection of their sets while keeping the elements of the sets private. The intersection is based on the matching of identifier keys. However, in a government setting, this is not enough due to the extreme data imbalance. Intersecting across many silos $\{\text{silos}^A \cap \text{silos}^B \cap \dots \cap \text{silos}^n\}$ will result in a very small set of data in each silo. For example, if silo A has a set of data with identifier keys 1,2,3,4,5, silo B has 3,5,6,8,9,10, and silo C has 3,4,5,6,7,8, then $\{\text{silos}^A \cap \text{silos}^B \cap \text{silos}^C\}$, based on PSI, consists of $\{3, 5\}$, which is much smaller than $\{\text{silos}^A \cup \text{silos}^B \cup \text{silos}^C\}$ which is equal to $\{1, 2, 3, 4, 5, 6, 7, 8, 9, 10\}$. Wei *et al.* [23] discuss PSI with specific ordered identifier keys (mentioned as ordered object identifier in our work) within FL. However, they require data with labels in a standard environment, which is not feasible in real-world cases. Our work is the first to implement the union concept $\{\text{silos}^A \cup \text{silos}^B \cup \text{silos}^C\}$ in vertical federated learning and address the issue of label costliness.

2.2 Learning on Non-IID Data Silos

Issues with data silos that are not identically distributed (Non-IID) [6] are often characterized by data and class size imbalances. This is especially true for real-world data, such as those from a tax office. In this case, economic conditions and taxpayer demographics can vary significantly from one region to another, resulting in data that is not identically distributed. To address this issue, Zhao *et al.* [27] proposed a representative learning approach for image data, but faced challenges in terms of accuracy. To overcome this, they proposed partial data sharing, which may not be compatible with the privacy-preserving nature of federated learning (FL). Wang *et al.* [22] also explored FL for Non-IID data silos, using rewards to incentivize silos with good accuracy. However, this approach requires a large number of weights to be stored, and the authors proposed dimension reduction to address this, which introduces uncertainty. Tzinis *et al.*[18] demonstrated that FL can be used for Non-IID data silos, proposing transfer learning as a solution. However, this requires a pre-trained model, which can be a black-box model with bias and inference from unknown trained data, which may not be suitable for a production environment such as a government sector.

2.3 Learning with label Costliness

Label costliness within vertical data silos leads to small data for collaborative model learning. Supervised learning is not recommended because it will lead to a model with high variance or bias, while unsupervised learning does not optimize available resources (label). A solution such as contrastive learning, as explored in studies [26, 16, 3], is designed for image/text/speech data [5]. Those data have properties of semantic relationships. When applied to tabular data, contrastive learning aims to cluster the tabular data unsupervisedly. Although there is limited research on the use of this algorithm within the context of tabular data, the work presented by [19] serves as an example that directly applies the concept of contrastive learning to tabular data. This current work recommends using partial data augmentation for tabular contrastive learning, which is similar to the method introduced by [4]. However, the current work did not support learning of data silos and failed in an extreme case of unbalanced data. It is worth mentioning that the foundation of our codebase was built upon the work of [19] but with substantial enhancements and refinements.

3 Problem Formulation

3.1 Definition

Definition 1: Tabular data A tuple $R_i = \{(x_i, y_i) | x \in \mathcal{R}^d, y \in \mathcal{R}^{d_0}, d > 0, i > 0\}$ is a set of type spaces (x, y) with d as the input dimension, d_0 as the output dimension, and i as a unique identifier key. The tabular data $\mathcal{D} = \{R_i\}$ is a collection of tuples R with unique object identifiers i , which can be expressed as $\mathcal{D} = \{\{(x_i, y_i)\}\}$. During the training of a model, a subset $\mathcal{X} \subset \mathcal{D}$ is taken, for example, if $R_1 = \{a_1, a_2, a_3, a_4, a_5, yes\}$, $R_2 = \{b_1, b_2, b_3, b_4, b_5, no\}$ and $R_3 = \{c_1, c_2, c_3, c_4, c_5, no\}$ then $\mathcal{D} = \{R_1, R_2, R_3\}$ which can be written as

$$\mathcal{D} = \begin{bmatrix} R_1 \\ R_2 \\ R_3 \end{bmatrix} = \begin{bmatrix} a_1, a_2, a_3, a_4, a_5, yes \\ b_1, b_2, b_3, b_4, b_5, no \\ c_1, c_2, c_3, c_4, c_5, no \end{bmatrix}$$

, and \mathcal{X} can be expressed as

$$\mathcal{X} = \begin{bmatrix} R_1 \\ R_2 \end{bmatrix} = \begin{bmatrix} a_1, a_2, a_3, a_4, a_5, yes \\ b_1, b_2, b_3, b_4, b_5, no \end{bmatrix}$$

Definition 2: Data silos A data silo that stores tabular data, $\mathcal{D}^n = \{R_i^n | n > 0, i > 0\}$, is indicated by the number n . For instance, $\mathcal{D}^1 = \{R_1, R_2, R_3\}$ implies that the first silo contains D data which is composed of the tuples R_1, R_2 and R_3 .

Definition 3: Silo space. Our work is based on the assumption that the data in each silo is vertically partitioned and connected across silos through quasi-identifier keys. This implies that the global business process has (imaginary) global data $T = \{(x_i^G, y_i^G)\}$. In reality, however, the data is divided into silos. Therefore, $T = \{\{\{R_i^n\}, y_i^G\}\} = \{\{\{\{(x_i, y_i)\}\}, y_i^G\}\}$ is composed of a set of tuples R from silos D^n with identifier keys i . This can be expressed as $T = \{\{\{D^n\}, Y^G\}\}$ where Y^G is the label of global data. Our use case holds $y_i = y_i^G$. If we let $G = \{D^n\} = \{\{R_i\}\}$ and $Y^G = \{y_i^G\}$, then the global data can be defined as $T = (G, Y^G)$. An example of this is shown in Figure 3.

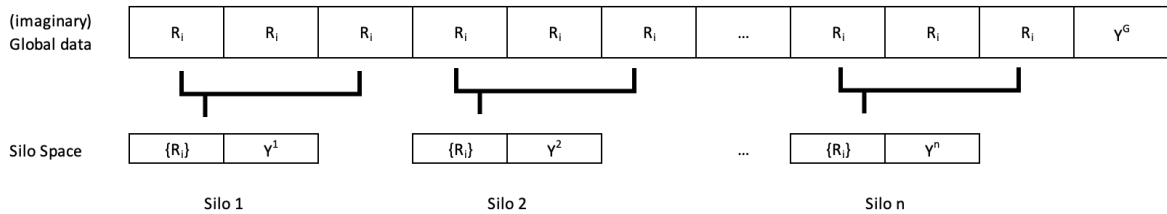


Figure 3: The (imaginary) global data and the silo space. Data are partitioned vertically, where $Y^G = Y^n$.

Definition 4: Same ordered object identifier key method Our method assumes that each silo contains the same data. Let $I = \langle ii \in \mathcal{N} \rangle$ be a set of unique identifiers i with a certain random order and I^n be a set of ordered i in silo n . Our method requires that $I^1 = I^2 = I^\dots = I^n$. The order is randomly generated but consistently per batch for all silos during learning. For example, when data with sequences of ID $I = \{1, 5, 6, 2, 8\}$ is needed for training, then a set of $\langle \mathcal{D}^n \rangle_I = \{R_1^n, R_5^n, R_6^n, R_2^n, R_8^n\}$ is taken. Within each silo, the data is trained consistently in the order of I . Let $\langle \mathcal{D}^n \rangle_I$ be \mathcal{D}^n ordered by I , then the assumption $T = \{(\mathcal{D}^n, Y^T)\}$ can be achieved when $\langle T \rangle_I = \{(\langle \mathcal{D}^n \rangle_I, \langle Y^T \rangle_I)\}$. Note that slice $\mathcal{X} \subset \mathcal{D}$, thus $\langle \mathcal{X} \rangle_I \subset \langle \mathcal{D} \rangle_I$. This uniformity is accomplished by synchronizing the random seed for each silo or client. The last definition is essential because our CFL applies contrastive learning in a silo for local learning. Contrastive learning loss, denoted by ℓ , is calculated by measuring the distances between the representations of an object reflected within weight ω . When brought to FL, in our CFL, the aggregation of ω on the global server is carried out assuming that each ω from each silo is from the same global object.

3.2 Problem Statement

In this section, we first explain the issue at hand, followed by a brief overview of the components of our CFL. Specifically, we discuss the core model. We use the case of the Indonesian Taxation Office as a data authority to illustrate how the model can be used to aggregate the risk of taxpayers. The model in our example is based on multiple data silos of business processes, which present the issues discussed in this paper. The model in our example has the (imaginary) global data, which, in reality, is composed of data silos.

3.2.1 Learning Tabular Data Silos with Vertical partition

The global business process has (imaginary) global data $T = (G, Y^G)$. The global business process aims to build $f : G \rightarrow Y^G$, where Y^G is the global label. Due to the silos environment, this can be formulated as $f : \{\mathcal{D}^n\} \rightarrow Y^G$. However, the acquisition of \mathcal{D}^n from other silos cannot be guaranteed due to privacy. FL can be proposed for this. In FL $f : (\mathcal{D}^n, \ell) \approx f : \{\mathcal{D}^n\} \rightarrow Y^G$ where $\ell(\cdot) = f(\cdot; \omega^G)$ is the loss function of FL given global parameters ω^G . The global parameter $\omega^G = \frac{1}{N} \sum_n \omega^n$ where ω^n is a silo parameter n . However, our use case deals with tabular non-IID data silos possessed vertical partition. Within these conditions, there are issues related to ω^G and ω^n . Although ω^n can be calculated, calculating ω^G is impractical. This is because, due to privacy, attributes within the vertical partition are unexposed outside the silo. We can see it as black-box vertical federated learning. Direct aggregation between ω^n , as proposed in horizontal FL, is wrong because each ω^n comes from different sets of attributes. Our first problem is to build an FL that comes from silos with vertical partitions without sacrificing privacy. The next issue concerns data availability, which will be discussed later.

3.2.2 Learning on Data Silos with Data Imbalance

Our next issue is data imbalance caused by the non-IID properties of the data silo and the label costliness. Data imbalance occurs in two forms: data size imbalance and class size imbalance. Due to this, the satisfaction of $I^1 = I^2 = I^\dots = I^n$ cannot be guaranteed during FL training. Following the above example, when $I = \{1, 5, 6, 2, 8\}$ is required for training, due to data size imbalance, when silo n^{th} does not have these data, or in some cases the member of I partially exists. The $f : (\mathcal{D}^n, \ell)$ cannot be calculated because $\langle \mathcal{D}^n \rangle_I$ do not exist or are partially exists. Local weight ω^n cannot be generated, which causes FL to fail to generate ω^G . Our second problem is to calculate ω^n and ω^T within a silo with a data imbalance scenario.

4 Proposed Method

4.1 Null Representation for Data Imbalance

This method is introduced to guarantee that $I^1 = I^2 = I^\dots = I^n$ is satisfied during training. When data from each silo is joined together ($D^1 \bowtie D^2 \bowtie \dots \bowtie D^n$), it creates an inner join or is called an intersect, as suggested by PSI. However, by applying the null representation approach during training,

an outer join ($D^1 \bowtie D^2 \bowtie \dots \bowtie D^n$) can be achieved. This also ensures that ω^n can always be calculated in local learning. The aim is to make sure that I is always available.

Empty (Null) data are essential to relational database theory, and CFL tries to keep it. When members of I^n partially or completely do not exist (null) in \mathcal{D}^n during training a model, data imputation can be implemented, e.g., statistical method (mean, median, mode) and tensor. However, our work proposes the use of null representations to represent empty data. Our CFL tries to keep the empty values by filling them with a 'zero' matrix. The rule is as follows:

$$R_i^n = \begin{cases} R_i^n, & \text{if } R_i \text{ is not null} \\ [0]^R, & \text{otherwise} \end{cases}$$

Applying this rule ensures $\langle \mathcal{D}^n \rangle_I = \{R_i^n\}$ to always be available in each silo. This method answers the nature of our extreme experiment settings. In some of our experiment settings, we left only 25% of the data in some silos with class and size imbalances. This is to demonstrate the non-IID and label costliness that exist in some silos. During local learning, there is a 75% chance that the slice $\langle \mathcal{X} \rangle_I$ does not exist in a silo such that $\mathcal{X} = [null]^X$. The application of tensor and statistical methods is impractical under such conditions. A similar treatment also works when the requested slice $\langle \mathcal{X} \rangle_I$ is partially available. For example, if data with object identifier $i = 2$ exists in the first silo but is absent in the second silo, during training, the second silo is trained with a zero matrix representing $i = 2$ in silo 2. The matrix below was the result of the above example:

$$\begin{bmatrix} R_1^1 \\ R_5^1 \\ R_2^1 \\ R_6^1 \end{bmatrix} = \begin{bmatrix} x_1^1 & x_1^1 & x_1^1 & x_1^1 & x_1^1 \\ x_5^1 & x_5^1 & x_5^1 & x_5^1 & x_5^1 \\ - & - & - & - & - \\ x_6^1 & x_6^1 & x_6^1 & x_6^1 & x_6^1 \end{bmatrix} = \begin{bmatrix} x_1^1 & x_1^1 & x_1^1 & x_1^1 & x_1^1 \\ x_5^1 & x_5^1 & x_5^1 & x_5^1 & x_5^1 \\ 0.0 & 0.0 & 0.0 & 0.0 & 0.0 \\ x_6^1 & x_6^1 & x_6^1 & x_6^1 & x_6^1 \end{bmatrix}$$

Our experiments have shown positive results using this method.

4.2 Tuple Representation for Tabular Contrastive Learning

A data silos environment is beneficial for machine learning. Knowledge from other silos can be used to enhance a model. To support machine learning in tabular data silos with non-IID and label costliness, we propose using contrastive learning with tuple representation as shown in our CFL, as demonstrated in Figure 2. The tuple representation approach aligns closely with the principles of contrastive learning for image data outlined by [25]. First, in each silo, our CFL replicates the data to create the representation required for contrastive learning. Let $\mathcal{X} \subseteq \mathcal{D}^n$ be a slice of data used in a local contrastive learning step, and then \mathcal{X} is cloned into two objects denoted $[x_i]$ and $[x_j]$, so $\mathcal{X} \rightarrow \{([x_i], [x_j])\}$. Each $[x]$ is cloned once more to form $[[x_i^a], [x_i^b]], ([x_j^a], [x_j^b])$. Each $[x]$ is an object for later modification of the representation calculation. Second, while $[x^b]$ is subjected to binomial noise and additional modifications, such as swapping or introducing Gaussian noise, each $[x^a]$ undergoes binomial noise

application exclusively. The noise rate is $z = \begin{cases} z, & \text{if } x_i \\ 1 - z, & \text{otherwise} \end{cases}$. Third, all $([x^a], [x^b])$ from each

pair are then inputted into the contrastive learning encoder and decoder layers. Let $\bar{E}(\cdot; \omega^e)$ be an encoder function given the parameter ω^e and $\bar{D}(\cdot; \omega^d)$ be the decoder function given parameter ω^d ; within contrastive learning in each silo, the aim is to minimize total loss L_t . For each representation object, apply $[x_{i,j}^{a,b}]' = \bar{D}(\bar{E}([x_{i,j}^{a,b}]; \omega^e); \omega^d)$. Both i, j are always transformed. For that we mention $([x_{i,j}^{a,b}]')$ as $([x'^a], [x'^b])$ in our work. The L_t is calculated as follows:

$$L_t([x'^a], [x'^b]) = (L_r([x'^a], [x'^b]) + L_c([x'^a], [x'^b]) + L_d([x'^a], [x'^b])) \quad (1)$$

Where L_r is the reconstruction loss, L_c is the contrastive loss, and L_d is the distance loss. The objective of contrastive learning is to minimize the total loss L_t .

$$\arg \min L_t(\mathcal{X}; \omega^e, \omega^d) = \arg \min \frac{1}{j} \sum_i^j L_t(\bar{D}(\bar{E}([x^a], [x^b]); \omega^e); \omega^d)$$

also can be written as (2)

$$L_t(\cdot; \omega^e, \omega^d) = f(\bar{E}(\cdot; \omega^e), \bar{D}(\cdot; \omega^d))$$

When $MSE(\cdot)$ is the mean square error function and $C(\cdot)$ is Euclidean distance function, then:

$$\begin{aligned}
 L_r([x'^a], [x'^b]) &= \frac{1}{N} \sum_n^N MSE([x'^a], [x'^b]) \\
 L_d([x'^a], [x'^b]) &= \frac{1}{N} \sum_n^N C([x'^a], [x'^b]) \\
 L_c([x'^a], [x'^b]) &= \frac{1}{N} \sum_n^N [x'^a] \cdot [x'^b]
 \end{aligned}
 \tag{3}$$

Although contrastive learning consists of two objects, an encoder and a decoder, after the whole contrastive learning is finished, only the encoder is used to transform the original data. The transformed data have better accuracy for supervised learning. The pseudocode for data generation can be found in Algorithm 1.

4.3 Tabular Contrastive Learning

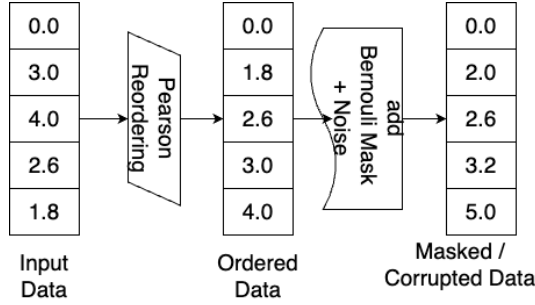


Figure 4: Data pre-processing as part of contrastive learning. To get the semantic relation, the data are ordered with Pearson Correlation. Then, the data are introduced with noise. This is required for contrastive learning

To obtain semantic relationship properties in our tabular data, we propose a Pearson Ordering/Sorting as part of the data pre-processing, see Figure 4. Pearson correlation is a statistic used to calculate the strength and direction of the linear relationship between two continuous variables. Let P be the Pearson correlation and \mathcal{D}' be the sorted/ordered data, then Pearson reordering $\mathcal{D}' = \text{sort}(P(\mathcal{D}))$ is achieved by sorting the Pearson correlation value. This was done on the assumption that we never

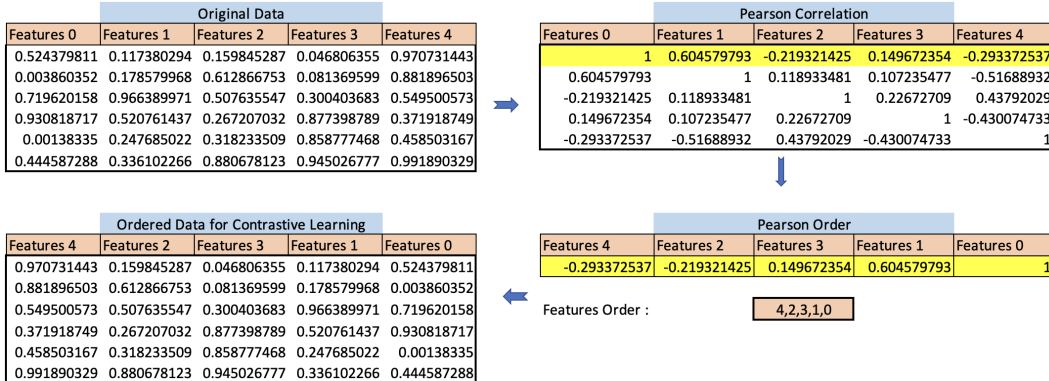


Figure 5: Our Pearson Ordering Processes. The original data are ordered by their Pearson Correlation value to get a semantic representation useful for contrastive learning. This is to get a horizontal semantic relationship

knew the actual semantic order of the data. $\mathcal{D} \leftarrow \mathcal{D}'$ is the data that will be used for contrastive learning. Our experiments show that Pearson reordering can increase the accuracy of contrastive learning. Figures 5 show how the reordering / sorting was carried out.

Algorithm 1 Generate noisy representation x_i and x_j

Input: $\mathcal{X}^n \subseteq \mathcal{D}^n$

Output: noisy representation of \mathcal{X}

$n > 2$
 $noiseRate = 0 < i < 1$
 $noiseCheck = True$
representations = $\mathcal{X} \rightarrow \{([x_i], [x_j])\} \rightarrow$
 $[[x_i^a], [x_i^b]], ([x_j^a], [x_j^b])]$

for item in representations **do**
 noiseCheck = not noiseCheck
 if noiseCheck **then**
 noises = noiseRate
 else
 noises = 1 - noiseRate
 end if
 $[x_{i/j}^a] = \text{BinomialNoise}([x_{i/j}^a], \text{noises})$
 $[x_{i/j}^b] = \text{BinomialNoise}([x_{i/j}^b], \text{noises}) +$
 $\text{GaussianNoise}(x_{i/j}^b, \text{noises})$
end for
return $[[x_i^a], [x_i^b]], ([x_j^a], [x_j^b])]$

Algorithm 2 Contrastive Federated Learning

Input: \mathcal{D}^n

Output: Encoder $\bar{E}(\cdot; \omega^e)$ from FL

Server: begin training
 Sends random seed

Silo: start training contrastive learning
 if $(\omega^{eG}, \omega^{dG})$ received from server **then**
 $f(\bar{E}(\cdot; \omega^e), \bar{D}(\cdot; \omega^d)) \leftarrow (\omega^e, \omega^d) \leftarrow$
 $(\omega^{eG}, \omega^{dG})$
 Back propagation
 end if
 Start quasi identifier match
 Draw data $\langle \mathcal{X}^n \rangle_I | \mathcal{X}^n \subseteq \mathcal{D}^n$
 for data R_i in $\langle \mathcal{X}^n \rangle_I$ **do**
 if data R_i do not exist **then**
 $R_i = [0.0, 0.0, \dots, 0.0]$
 end if
 Generate noisy representation
 $[[x_i^a], [x_i^b]], ([x_j^a], [x_j^b])]$
 Loss $L_t(\cdot; \omega^e, \omega^d) = f(\bar{E}(\cdot; \omega^e), \bar{D}(\cdot; \omega^d))$
 Send (ω^e, ω^d) to the server
 end for

Server: Federated Average
 Receive (ω^e, ω^d)
 Federated Average $F(g) = \frac{1}{N} \sum_n (\omega^e, \omega^d) \rightarrow$
 $(\omega^{eT}, \omega^{dT})$
 Send $(\omega^{eG}, \omega^{dG})$ back to clients

Clients: continue training
return $\bar{E}(\cdot; \omega^e)$

4.4 CFL Algorithm

Our CFL starts with building a contrastive learning model in each silo. This model is done by training data $\mathcal{D}^n \leftarrow \text{sort}(P(\mathcal{D}^n)) \leftarrow \langle \mathcal{D}^n \rangle_I$. The CFL consists of two objects: an encoder and a decoder. This is against the work proposed by Qi *et al.* [15] that works with vertical FL with contrastive learning for image data. That work proposes three encoders and decoders, which are very expensive to the network. This cost can be avoided by our CFL. The next step is still in the silo, where the CFL calculates the loss function of contrastive learning, defined as $L_t(\cdot; \omega^e, \omega^d) = f(\bar{E}(\cdot; \omega^e), \bar{D}(\cdot; \omega^d))$. Both the encoder and decoder parameters (ω^e, ω^d) are used for the FL part. Next, CFL does FL by aggregating the parameters (ω^e, ω^d) on the global server. The aggregation was carried out by averaging the parameters of each silo with a federated average (FedAVG) denoted as $F(g) = \frac{1}{n} \sum_1^n (\omega^e, \omega^d) \rightarrow (\omega^{eT}, \omega^{dT})$ where $(\omega^{eT}, \omega^{dT})$ are the global averaged parameters. The aggregated global parameters are then returned to each silo for back-propagation operations to continue contrastive learning.

Similarly to the existing proposed contrastive learning techniques, at the end of the learning loop, the header (decoder) is omitted, as illustrated early in Figure 1. Therefore, during supervised learning in each silo, the functions were originally $f : \mathcal{D} \rightarrow Y$ by performing contrastive learning, and it is expected $f : \bar{E}(\mathcal{D}^n; \omega^e) \rightarrow Y^n$. The expectation is $f : \bar{E}(\mathcal{D}; \omega^e) \approx f : T$ and $f : \bar{E}(\mathcal{D}; \omega^e)$ closer to the actual value Y^G than the original $f : \mathcal{D}$. The pseudocode of CFL can be found on Algorithm 2.

5 Experiments

Our experiments involve five datasets: Income, blog, Biometric Blender Synthetic, cifar10, and MNIST. Two of these datasets are image datasets (Cifar10 and MNIST), which are commonly used in many

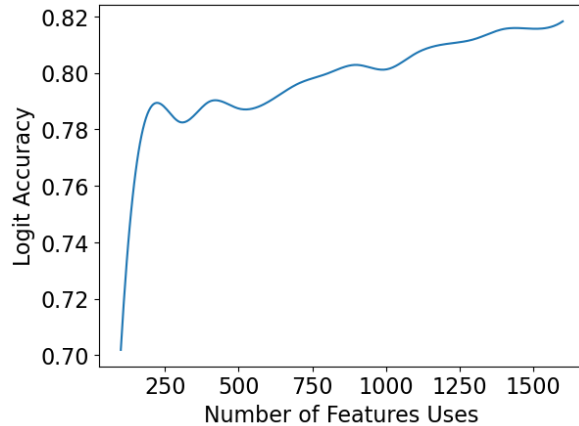


Figure 6: Accuracy on shuffled Biometric Blender Synthetic Datasets when the features are partially used.

experiments. To make them more suitable for our purposes, the columns in each dataset were randomly shuffled to simulate a tabular dataset and remove any semantic relations. The Biometric Blender Synthetic Dataset (BB) [17] is an ultrahigh-dimensional, multiclass synthetic data generator to mimic the biometric feature space. This was chosen because of its versatility to generate many features. We constructed a dataset consisting of 10 classes for BB, each row containing 1600 features. Figure 6 illustrates the impact of the feature count on the accuracy of logistic regression applied to this dataset. Table 1 shows the complete setup for every experiment conducted in this work. Logistic regression was used to compare the results of each experiment and obtain the accuracy. The training data rate was set to 0.3 and the validation data rate was set to 0.7. We could not set the training data to 0.1, as is usually done for contrastive learning experiments, due to data imbalances. For example, in our experiments, we applied a 0.5 data drop to a client, meaning that the intended client had $0.3 * 0.5 = 0.15$ training data. Although the data were shuffled at each epoch, the availability of certain data remained static. For example, if data $id = 2$ from the 2^{nd} silo did not exist in epoch one, then it did not exist in other epochs either.

Table 1: Experiments Setup

Dataset		cifar10	BlogFeedback	income	syn	cifar10
Rows		50000	52396	30162	99900	50000
Full Feats		1024	280	105	1600	1024
Normal Setting	Silos Count	4	4	5	4	4
	Encoder Size	256	256	256	2048	256
	Feats Size	256	70	21	400	256
Data Drop Settings	Silos Count	4	4	5	4	4
	Encoder Size	256	256	256	2048	256
	Feats Size	256	70	21	400	256
Class Imbalance Setting	Silos Count	4	4	5	4	4
	Encoder Size	256	256	256	2048	256
	Feats Size	256	70	21	400	256
Mixed Setting	Silos Count	16	4	5	16	16
	Encoder Size	256	256	256	2048	256
	Feats Size	64	70	21	100	64

5.1 Experiment Settings

Our main experiment environment is always within silo space, as required by our use case. The existing contrastive algorithm for tabular data, SubTab [20], will be evaluated with two methods: FL and non-FL. The SubTab is introduced with FL to adapt silo space, however, SubTab algorithm does not support silo space and data imbalance. We apply the same "null representation" method to support

the variation in data imbalance between silos.

Standard Lab Setting. We conducted our first experiment in a standard setting, which ensures data availability and avoids data imbalance. This is a typical approach for experiments, even though it does not reflect the most realistic environment. Nevertheless, it serves as a foundation for understanding the models.

Data Size Imbalance Setting. Our second setting establishes an imbalance in the data size within the silo space. The experiment was configured with a 0.25 client drop and a 0.5 data drop. This means that 25% of the total clients have a data size imbalance, that is, if the total number of clients is 4, then the first client has a data size imbalance. Clients with an imbalance of data size have only 50% of the data compared to others during training. Table 1 outlines the complete setup.

Class Size Imbalance Setting. Our third setting establishes an imbalance in the silo space with respect to class size. The experiment was set with a 0.25 client imbalance and a 0.5 class imbalance. This means that 25% of the total clients have a class size imbalance, i.e., if the total client count is 4, then the first client has a class size imbalance. Clients with class size imbalance have only 50% of the data in 50% of the randomly selected classes compared to the others during contrastive training and Logistic Regression Prediction. Table 1 outlines the complete setup.

Mixed Case Settings. The last experiment was designed with an unequal distribution of data and classes. A 0.25 client drop and a 0.5 data drop were implemented, as well as a 0.25 client imbalance and a 0.5 class imbalance. The first 25% of total clients were affected by the data drop, while the next 25% of total clients experienced the class imbalance.

6 Result and Evaluation

For each experiment, we generate line graphs that illustrate the differences in accuracy between the predicted labels in each silo and the actual labels from the (imaginary) global dataset. Our goal is to train a model within a silo $f : D \rightarrow Y$ that has accuracy similar to that of a model trained with the (imaginary) global dataset $f : T \rightarrow Y^G$. The accuracy delta, denoted as $f : \mathcal{D}^n \triangleq f : T \rightarrow Y^G$, is represented by the graphs. The smaller the reading, the closer it is to the actual label from global data. For instance, a 0.01 on the graph implies that $(\mathcal{A}(f : T) - \mathcal{A}(f : \bar{E}(\mathcal{D}; \omega^e))) = 0,01$, where $\mathcal{A}(\cdot)$ is a model accuracy function. If the chart displays a negative value, it indicates that $\mathcal{A}(f : T) < \mathcal{A}(f : \bar{E}(\mathcal{D}; \omega^e))$.

Each graph has four lines: SubTab, SubTab FL, LL, and CFL. The SubTab line shows the difference in accuracy between Subtab without FL and logistic regression on the (imaginary) global data, denoted as $f : \bar{E}(\mathcal{D}; \omega^e) \triangleq f : T$. The SubTab FL line shows the difference in accuracy between Subtab with FL and logistic regression in the (imaginary) global data, denoted as $f : \bar{E}(\mathcal{D}; \omega^{eT}) \triangleq f : T$. The LL line illustrates the difference in accuracy between local logistic regression trained in a silo and the logistic regression in the (imaginary) global data, denoted as $f : \mathcal{D}^n \triangleq f : T$. The CFL line shows the difference in accuracy between the CFL and logistic regression in the (imaginary) global data, denoted as $f : \bar{E}(\mathcal{D}; \omega^{eT}) \triangleq f : T$.

6.1 Multiple Settings' Result

6.1.1 Lab Setting

Experiments conducted in a standard lab setting demonstrate that the accuracy of our proposed CFL is closest to the accuracy of the (imaginary) global model $f : T \rightarrow Y^G$ among all five datasets. Figure 8 illustrates the results. Applying FL to existing SubTab decreases performance, which is expected since the original SubTab does not support FL. The SubTab without FL $f : \bar{E}(\mathcal{D}; \omega^e)$ performs worse than local logistic regression $f : \mathcal{D}^n$ in this setting. Figure 7 displays the loss synchronizations of CFL in a client resulting from federated learning. The loss graph indicates that the CFL algorithm takes a considerable amount of time to stabilize. The overall result is summarized in Table 2.

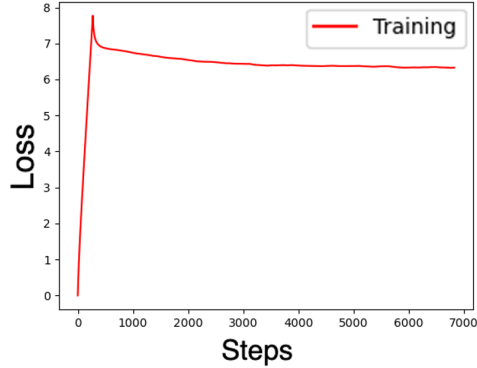


Figure 7: Loss synchronization on the ‘Standard Lab Setting’. In the early stages, the loss has a very low value. However, the loss is stable after around 200 steps.

Table 2: Delta Accuracy between (imaginary) global data model and models trained in each silo within a standard lab setting. The values presented are the mean of each model. The smaller the better.

Dataset	SubTab	SubtTab FL	LL	CFL(ours)
blog	0.055018	0.054293	0.050978	0.031708
cifar10	0.001155	0.017382	0.001602	-0.019631
income	0.044693	0.048340	0.063178	0.041264
mnist	0.080187	0.162956	0.075360	0.040467
syn	0.280015	0.488859	0.048538	0.045176

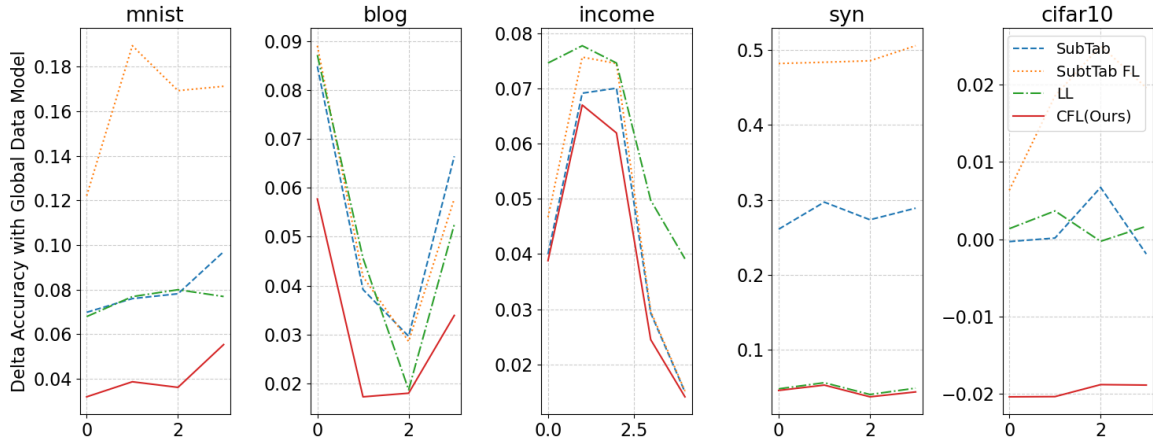


Figure 8: Delta Accuracy between (imaginary) global data model $f : T$ and models ($f : \mathcal{D}^n$ or $f : (\mathcal{D}^n, \omega)$) trained in each silo within a standard lab setting. The smaller/lower the better.

6.1.2 Data Size Imbalance Setting

By decreasing the number of clients by 25%, the same outcome was achieved. As demonstrated in Figure 9. Table 3 displays the difference in accuracy with this configuration. The results were comparable to those of the standard lab setting.

Table 3: Delta Accuracy between (imaginary) global data model and models trained in each silo. This setting has clients with small sizes compared to others. The 1st client has only 25% of the data size. The values presented are the mean of each model. The smaller the better.

Dataset	SubTab	SubtTab FL	LL	CFL(ours)
blog	0.053314	0.052041	0.047216	0.035449
cifar10	0.002058	0.018772	0.003059	-0.019596
income	0.046001	0.050040	0.063178	0.039364
mnist	0.084251	0.166638	0.078847	0.029719
syn	0.282343	0.493576	0.050099	0.046745

Table 4: Delta Accuracy between (imaginary) global data model and models trained in each silo. This setting has a client with an imbalance class. For MNIST, the 1st client has 10 classes, with 5 classes only 50% data compared to the others. The values presented are the mean of each model. The smaller the better.

Dataset	SubTab	SubtTab FL	LL	CFL(ours)
blog	0.051226	0.047838	0.047367	0.033028
cifar10	0.013048	0.030048	0.010585	-0.007769
income	0.050794	0.052274	0.063178	0.045566
mnist	0.094748	0.193256	0.096982	0.031846
syn	0.312663	0.501024	0.067341	0.059696

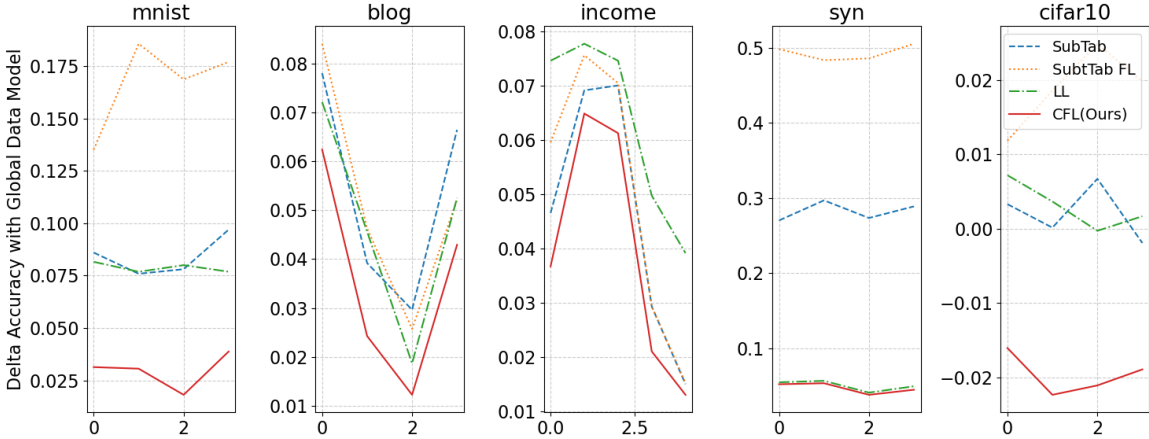


Figure 9: Delta Accuracy between (imaginary) global data model $f : T$ and models ($f : \mathcal{D}^n$ or $f : (\mathcal{D}^n, \omega)$) trained in each silo within a non-standard setting. These settings have an imbalance of data size. The smaller/lower the better.

6.1.3 Class Size Imbalance Setting

The proposed CFL yields 1%-5% better performance than the previous settings when class imbalance is taken into account. As seen in Figure 10, the deltas are smaller, indicating that the accuracy of $f : T$ is closer. Table 4 shows the mean accuracy delta in this setting. This is expected, as FL allows for more knowledge to be gained from other silos.

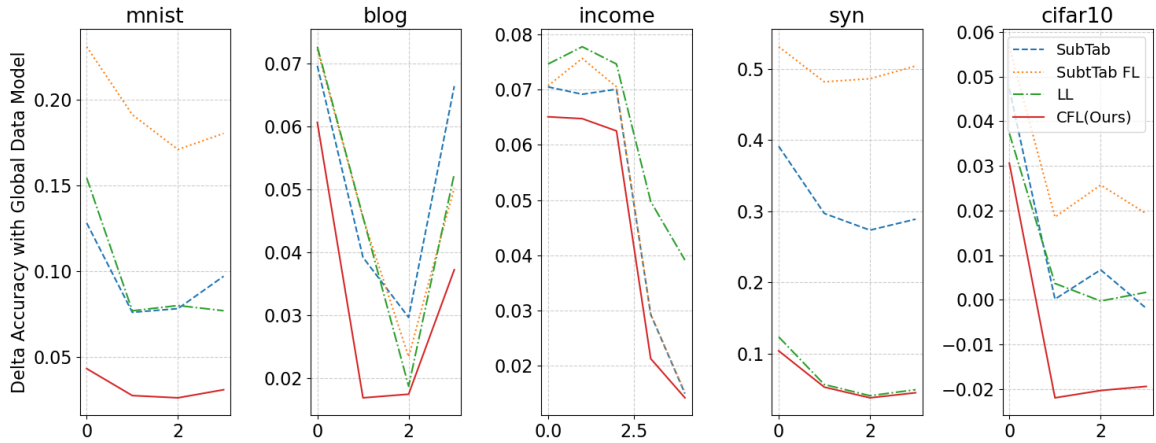


Figure 10: Delta Accuracy between (imaginary) global data model $f : T$ and models ($f : \mathcal{D}^n$ or $f : (\mathcal{D}^n, \omega)$) trained in each silo within a non-standard setting. These settings have a class size imbalance. The smaller / lower, the better.

6.1.4 Mixed Case Settings

In this setting, the proposed algorithm, CFL, is particularly effective. We set up 16 clients with MNIST, CIFAR10, and Biometric Blender synthetic data, with Blog and Income having 4 and 5 clients respectively. Each of these clients was introduced with data and class imbalance. As Figure 11 shows, more complex environments give smaller deltas to our CFL. The mean of the results can be seen in Table 5.

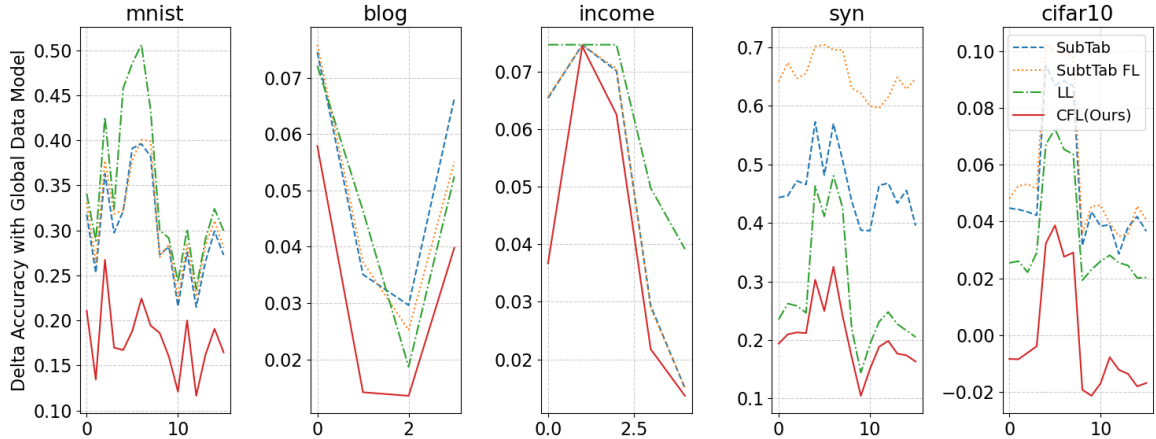


Figure 11: Delta Accuracy between (imaginary) global data model $f : T$ and models ($f : \mathcal{D}^n$ or $f : (\mathcal{D}^n, \omega)$) trained in each silo within a non-standard setting. These settings have data and class size imbalances. The smaller/lower the better.

6.2 Effects of the Pearson Reordering

We proposed a simple Pearson reordering method in our experiment, which was conducted in a standard laboratory setting. This method was able to increase accuracy on datasets that both CFL and SubTab had difficulty improving performance on, such as blog and Biometric Blender synthetic. Applying Pearson Reordering, CFL performed better on both datasets. However, we did not conduct

Table 5: Delta Accuracy between (imaginary) global data model and models trained in each silo. This setting has both a data size imbalance and a class imbalance in the silo space. The values presented are the mean of each model. The smaller the better.

Dataset	SubTab	SubTab FL	LL	CFL(ours)
blog	0.051370	0.048338	0.047408	0.031343
cifar10	0.051974	0.057927	0.034902	-0.001574
income	0.050852	0.050937	0.062551	0.041795
mnist	0.301237	0.309816	0.346625	0.178564
syn	0.461634	0.649977	0.279089	0.204482

Table 6: Delta accuracy when Pearson Reordering is applied under lab setting.

Dataset	CFL with Pearson	CFL No Pearson	Delta Accuracy
blog	0.778451	0.777247	0.001204
cifar10	0.317117	0.318747	-0.001630
income	0.782928	0.785060	-0.002132
mnist	0.833200	0.852551	-0.019352
syn	0.824907	0.747374	0.077533

a comprehensive study on Pearson reordering to fit certain characteristics of the data set. Table 6 displays the performance of Pearson reordering.

6.3 Evaluation

The Contrastive Federated Learning for Tabular Data Silos (CFL) algorithm has been shown to outperform local logistic regression and other existing contrastive learning for tabular data algorithms. Our experiments have demonstrated that it is capable of performing well in extreme settings as encountered in the real world. Figure 12 illustrates that CFL is capable of adapting to any kind of situation. Furthermore, this paper has demonstrated that "Pearson Reordering" can improve the contrastive algorithm in a variety of scenarios.

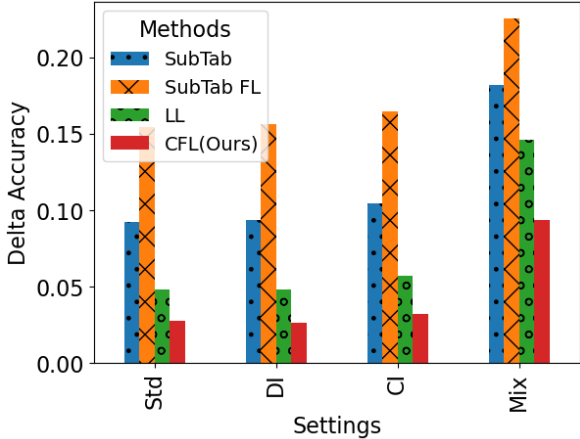


Figure 12: Overall delta accuracy in each setting. Deltas measure how close models ($f : \mathcal{D}^n$ or $f : (\mathcal{D}^n, \omega)$) are to $f : T$. The smallest is the best. Std is standard lab setting, DI is data imbalance setting, CI is the class imbalance setting, and Mix is DI + CI.

7 Conclusion

Challenges like non-IID data and the high cost of labeling arise within government data silos primarily due to the inherent characteristics of government operations. However, these challenges are manifested in certain real-world scenarios, where the same objects are referred to by different identifiers in different

applications. Our CFL offers an approach to learning tabular data from data silos and we are the first to present an integrated solution. Our CFL is able to adapt and gain accuracy in a very complex situation. For future studies, the nature of the result of our CFL can be used with multi-model data silos.

8 Acknowledgement

This work acknowledges the funds provided by the Indonesia Endowment Funds for Education and the support from the Indonesian Taxation Office and the University of Queensland, Australia.

9 Declaration of generative AI and AI-assisted technologies in the writing process

During the preparation of this work, the author(s) used Writefull and Grammarly to enhance readability. After using this tool/service, the author(s) reviewed and edited the content as needed and take(s) full responsibility for the content of the publication.

References

- [1] N. Bouacida and P. Mohapatra. Vulnerabilities in federated learning. *IEEE Access*, 9:63229–63249, 2021.
- [2] T. Chen, X. Jin, Y. Sun, and W. Yin. Vaff: a method of vertical asynchronous federated learning. *arXiv preprint arXiv:2007.06081*, 2020.
- [3] T. Chen, S. Kornblith, M. Norouzi, and G. Hinton. A simple framework for contrastive learning of visual representations. In *International conference on machine learning*, pages 1597–1607. PMLR, 2020.
- [4] Y. Chen, Y. Ning, M. Slawski, and H. Rangwala. Asynchronous online federated learning for edge devices with non-iid data. *Proceedings - 2020 IEEE International Conference on Big Data, Big Data 2020*, pages 15–24, 12 2020. online learning with multiple clients.update global model without wait others.
- [5] M. Gutmann and A. Hyvärinen. Noise-contrastive estimation: A new estimation principle for unnormalized statistical models. In *Proceedings of the thirteenth international conference on artificial intelligence and statistics*, pages 297–304. JMLR Workshop and Conference Proceedings, 2010.
- [6] K. Hsieh, A. Phanishayee, O. Mutlu, and P. Gibbons. The non-iid data quagmire of decentralized machine learning. In *International Conference on Machine Learning*, pages 4387–4398. PMLR, 2020.
- [7] Y. Ji and L. Chen. Fedqnn: A computation-communication-efficient federated learning framework for iot with low-bitwidth neural network quantization. *IEEE Internet of Things Journal*, 10:2494–2507, 2 2023.
- [8] T. Kipf, E. van der Pol, and M. Welling. Contrastive learning of structured world models. *8th International Conference on Learning Representations, ICLR 2020*, 11 2019.
- [9] L. Liu, J. Zhang, S. H. Song, and K. B. Letaief. Client-edge-cloud hierarchical federated learning. *IEEE International Conference on Communications*, 2020-June, 5 2019. combine cloud FL and edge FL.
- [10] L. Lu and N. Ding. Multi-party private set intersection in vertical federated learning. *Proceedings - 2020 IEEE 19th International Conference on Trust, Security and Privacy in Computing and Communications, TrustCom 2020*, pages 707–714, 12 2020.

- [11] X. Lu, Y. Liao, P. Lio, and P. Hui. Privacy-preserving asynchronous federated learning mechanism for edge network computing. *IEEE Access*, 8:48970–48981, 2020. Fog Computing. Asynchronous Federated Learning with Dual-WeightsCorrection.
- [12] B. McMahan, E. Moore, D. Ramage, S. Hampson, and B. A. y Arcas. Communication-efficient learning of deep networks from decentralized data. In *Artificial intelligence and statistics*, pages 1273–1282. PMLR, 2017.
- [13] MoFan, HaddadiHamed, KatevasKleomenis, MarinEduard, PerinoDiego, and KourtellisNicolas. Ppfl. *GetMobile: Mobile Computing and Communications*, 25:35–38, 3 2022. Attack on Federated learning with confidential computing.
- [14] R. Motwani and Y. Xu. Efficient algorithms for masking and finding quasi-identifiers. In *Proceedings of the Conference on Very Large Data Bases (VLDB)*, pages 83–93, 2007.
- [15] T. Qi, F. Wu, C. Wu, L. Lyu, T. Xu, H. Liao, Z. Yang, Y. Huang, and X. Xie. Fairvfl: A fair vertical federated learning framework with contrastive adversarial learning. *Advances in Neural Information Processing Systems*, 35:7852–7865, 12 2022.
- [16] M. Servetnyk, C. C. Fung, and Z. Han. Unsupervised federated learning for unbalanced data. *2020 IEEE Global Communications Conference, GLOBECOM 2020 - Proceedings*, 2020-January, 2020.
- [17] M. Stippinger, D. Hanák, M. T. Kurbucz, G. Hanczár, O. M. Törteli, and Z. Somogyvári. Biometricblender: Ultra-high dimensional, multi-class synthetic data generator to imitate biometric feature space. *SoftwareX*, 22:101366, 2023.
- [18] E. Tzinis, J. Casebeer, Z. Wang, and P. Smaragdis. Separate but together: Unsupervised federated learning for speech enhancement from non-iid data. *IEEE Workshop on Applications of Signal Processing to Audio and Acoustics*, 2021-October:46–50, 2021.
- [19] T. Ucar. SubTab: Subsetting Features of Tabular Data for Self-Supervised Representation Learning. <https://github.com/AstraZeneca/SubTab>, June since 2021.
- [20] T. Ucar, E. Hajiramezanali, and L. Edwards. Subtab: Subsetting features of tabular data for self-supervised representation learning. *Advances in Neural Information Processing Systems*, 34, 2021.
- [21] H. Wang, Z. Kaplan, D. Niu, and B. Li. Optimizing federated learning on non-iid data with reinforcement learning. *Proceedings - IEEE INFOCOM*, 2020-July:1698–1707, 7 2020.
- [22] L. Wang, B. Lei, Q. Li, H. Su, J. Zhu, and Y. Zhong. Triple-memory networks: A brain-inspired method for continual learning. *IEEE Transactions on Neural Networks and Learning Systems*, 33:1925–1934, 5 2022. continue learning try to overcome catastrophic forgetting. mimics the works of brain.
- [23] K. Wei, J. Li, C. Ma, M. Ding, S. Wei, F. Wu, G. Chen, and T. Ranbaduge. Vertical federated learning: Challenges, methodologies and experiments. *arXiv preprint arXiv:2202.04309*, 2022.
- [24] S. Yang, F. Wu, S. Tang, X. Gao, B. Yang, and G. Chen. On designing data quality-aware truth estimation and surplus sharing method for mobile crowdsensing. *IEEE Journal on Selected Areas in Communications*, 35:832–847, 4 2017.
- [25] Y. Yao, N. Desai, and M. Palaniswami. Masked contrastive representation learning. *arXiv preprint arXiv:2211.06012*, 11 2022.
- [26] F. Zhang, K. Kuang, L. Chen, Z. You, T. Shen, J. Xiao, Y. Zhang, C. Wu, F. Wu, Y. Zhuang, et al. Federated unsupervised representation learning. *Frontiers of Information Technology Electronic Engineering*, 24(8):1181–1193, 2023.
- [27] Y. Zhao, M. Li, L. Lai, N. Suda, D. Civin, and V. Chandra. Federated learning with non-iid data. *The Computer Journal*, 2018.

- [28] L. Zhou, R. Huang, and B. Li. “what is mine is not thine”: Understanding barriers to china’s interagency government data sharing from existing literature. *Library and Information Science Research*, 42:101031, 7 2020.